

# Testing Partonic Charge Symmetry at a High-Energy Electron Collider

T.J. Hobbs,<sup>1</sup> J. T. Londergan,<sup>1</sup> D.P. Murdock,<sup>2</sup> and A. W. Thomas<sup>3</sup>

<sup>1</sup>*Department of Physics and Center for Exploration of Energy and Matter,  
Indiana University, Bloomington, IN 47405, USA*

<sup>2</sup>*Department of Physics, Tennessee Technological University, Cookeville, TN 38505, USA*

<sup>3</sup>*CSSM, School of Chemistry and Physics, University of Adelaide, Adelaide, South Australia 5005, Australia*

We examine the possibility that one could measure partonic charge symmetry violation (CSV) by comparing neutrino or antineutrino production through charged-current reactions induced by electrons or positrons at a possible electron collider at the LHC. We calculate the magnitude of CSV that might be expected at such a facility. We show that this is likely to be a several percent effect, substantially larger than the typical CSV effects expected for partonic reactions.

PACS numbers: 12.15.+y, 13.15.+g, 24.85.+p

Charge symmetry is a very specific operation involving isospin, which leads to the interchange of protons and neutrons, or equivalently the interchange of up and down quarks. The charge symmetry operator  $P_{CS}$  corresponds to a rotation of  $180^\circ$  about the 2 axis in isospin space, such that

$$P_{CS} = e^{i\pi T_2}, \quad P_{CS}|u\rangle = -|d\rangle; \quad P_{CS}|d\rangle = |u\rangle. \quad (1)$$

It is of particular importance because at low energies, where it has been studied extensively, charge symmetry is a far better symmetry than isospin in general, typically being respected to better than 1% [1, 2]. It is therefore natural to assume that charge symmetry is also valid at the partonic level and, indeed, almost all analyses of parton distribution functions (PDFs) assume charge symmetry, whether the assumption is stated or not. The importance of charge symmetry violation in PDFs within the context of tests of the Standard Model has recently been of considerable interest [3, 4].

To date, no violation of charge symmetry has been observed at the partonic level, although the one global analysis that did allow for CSV did find a preferred solution with a non-zero effect – albeit with very large errors [5]. The current upper limits are consistent with the validity of partonic charge symmetry in the range 5-10% [6]. Theoretical models generally produce estimates of charge symmetry violation (CSV) in PDFs which for many observables give effects at roughly the 1% level [6, 7]. This presents a significant challenge for experimentalists, first to observe effects of this magnitude and then to isolate the signal from competing effects of similar size.

A new facility has recently been proposed that would collide electrons or positrons from an elec-

tron accelerator with protons or deuterons from the LHC [8]. In this paper we will show that such a facility (given the name LHeC) has the potential to produce charge symmetry violating effects which are considerably larger than those expected with other facilities. We will review the effect in question, show the results of theoretical calculations for the proposed CSV effects, and discuss why they ought to be expected to be relatively large at energies accessible to an electron-ion collider.

The reactions of interest are the charged current (CC) cross sections for electron and positron deep inelastic scattering at energies in the range 50-100 GeV on protons and deuterons at LHC energies, *i.e.*, several TeV. These are important because they directly and unambiguously probe the flavor structure of the proton PDFs in the valence region. Consider the deep inelastic reaction ( $e^-, \nu_e$ ). A high-energy electron incident on a proton produces a neutrino. The process results from a  $W^-$  which is absorbed on quarks from the proton, as shown schematically in Fig. 1; the final hadronic state is not observed. The signature for this process is disappearance of the electron, together with very large deposition of energy in the hadronic sector.

The  $F_2$  structure function for the CC reaction on a proton has the form

$$F_2^{W^-p}(x) = 2x[u(x) + c(x) + \bar{d}(x) + \bar{s}(x)]. \quad (2)$$

These reactions will occur at extremely high energies and very large  $Q^2$ . Therefore, any corrections to the  $F_2$  structure functions in Eqs. (2) and (3) arising from quark mixing matrices, quark masses or higher-twist effects should be completely negligible.

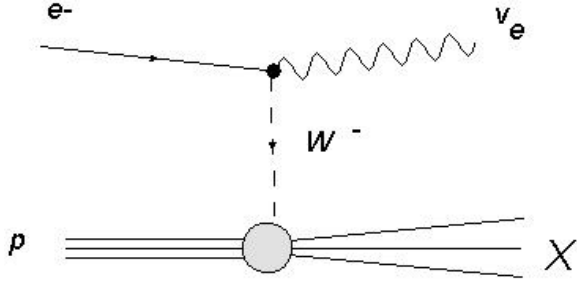


FIG. 1: Schematic picture of charged-current neutrino production in DIS induced by an electron on a proton.

We can also consider the corresponding reaction for positrons on protons,  $(e^+, \bar{\nu}_e)$ . This reaction involves the absorption of a  $W^+$  on the proton, with the resulting  $F_2$  structure function

$$F_2^{W^+p}(x) = 2x[\bar{u}(x) + \bar{c}(x) + d(x) + s(x)]. \quad (3)$$

We can straightforwardly calculate the  $F_2$  structure functions (per nucleon) on the deuteron,

$$\begin{aligned} F_2^{W^-D}(x) &= x[u^+(x) + d^+(x) + 2c(x) \\ &\quad + 2\bar{s}(x) - \delta d(x) - \delta \bar{u}(x)] ; \\ F_2^{W^+D}(x) &= x[u^+(x) + d^+(x) + 2\bar{c}(x) \\ &\quad + 2s(x) - \delta \bar{d}(x) - \delta u(x)] . \end{aligned} \quad (4)$$

In Eq. (4) we introduce combinations of quark parton distribution functions (PDFs) that are even or odd under charge conjugation, and the CSV PDFs

$$\begin{aligned} q^\pm(x) &= x[q(x) \pm \bar{q}(x)] ; \\ \delta u(x) &= u^p(x) - d^n(x) ; \\ \delta d(x) &= d^p(x) - u^n(x) . \end{aligned} \quad (5)$$

There are analogous relations to Eq. (5) for the antiquark CSV PDFs. For the remainder of this letter we assume that  $\bar{c}(x) = c(x)$ . The distributions  $q^-(x)$ , which involve the differences between quark and antiquark PDFs (alternatively, they are the  $C$ -odd combinations of quark distributions), are the *valence* parton distributions for a given quark flavor.

Now define the following quantity,

$$R^-(x) \equiv \frac{2(F_2^{W^-D}(x) - F_2^{W^+D}(x))}{F_2^{W^-p}(x) + F_2^{W^+p}(x)} . \quad (6)$$

The quantity  $R^-(x)$  is given by the difference in the  $F_2$  structure functions per nucleon for electron-deuteron and positron-deuteron CC reactions, divided by the average  $F_2$  structure function for CC

reactions on protons initiated by electrons and by positrons.

Using Eqs. (2), (3) and (4) we can straightforwardly show that the quantity  $R^-(x)$  in (6) has the form

$$R^-(x) = \frac{x[-2s^-(x) + \delta u^-(x) - \delta d^-(x)]}{x[u^+(x) + d^+(x) + s^+(x) + 2c(x)]} . \quad (7)$$

Thus  $R^-(x)$  is proportional to the valence quark CSV parton distributions plus the strange quark asymmetry (the difference between the strange and antistrange PDFs). Insofar as the strange quark asymmetry exists, it should be large only at quite small Bjorken  $x < 0.1$ , while theoretical estimates of the valence CSV parton distributions [9, 10] suggest that for  $Q^2 \sim 10 \text{ GeV}^2$  they peak at values  $x \sim 0.4$ .

Consider a hypothetical collider with 50 GeV electrons or positrons colliding with protons and deuterons of energy roughly 7 TeV. This would be similar to the possibilities if an electron collider were built at the LHC. Consider charged-current reactions at such a facility with  $Q^2 = 10^5 \text{ GeV}^2$ . We know of two different mechanisms for charge symmetry violation in parton distribution functions. The first arises from the radiation of a photon by a quark. Such contributions are shown schematically in Fig. 2; they were first calculated by the MRST group [11] and Gluck *et al.* [12]. These QED corrections are analogous to the coupling of gluons to quarks, except that photons do not have the self-coupling terms possessed by gluons. Inclusion of these ‘QED splitting’ terms will produce charge symmetry violation in parton distribution functions because of the electromagnetic (EM) coupling due to the different charges of up and down quarks.

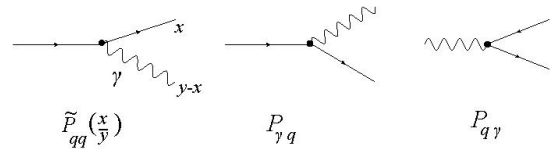


FIG. 2: Schematic picture of quarks coupling to photons. This gives the origin of QED splitting that produces CSV effects in parton distribution functions.

The behavior of parton distributions with increasing  $Q^2$  is given by the DGLAP evolution equations [13–15]. We expand the DGLAP evolution equations to lowest order in both the strong

coupling  $\alpha_s$  and the electromagnetic coupling  $\alpha$ ,

$$\begin{aligned}
\frac{\partial q_i(x, \mu^2)}{\partial \ln \mu^2} &= \frac{\alpha_s}{2\pi} [P_{qq} \otimes q_i + P_{qg} \otimes g] \\
&+ \frac{\alpha}{2\pi} e_i^2 \tilde{P}_{qq} \otimes q_i ; \\
\frac{\partial g(x, \mu^2)}{\partial \ln \mu^2} &= \frac{\alpha_s}{2\pi} \left[ \sum_j P_{gq} \otimes q_j + P_{gg} \otimes g \right] \\
&+ \frac{\alpha}{2\pi} e_i^2 \tilde{P}_{qq} \otimes q_i ; \\
\frac{\partial \gamma(x, \mu^2)}{\partial \ln \mu^2} &= \frac{\alpha}{2\pi} \sum_j e_j^2 P_{\gamma q} \otimes q_j . \tag{8}
\end{aligned}$$

In Eq. (8),  $q_i(x, \mu^2)$  is the parton distribution for a given flavor  $i$ ,  $g(x, \mu^2)$  is the gluon distribution and  $\gamma(x, \mu^2)$  is a “photon parton distribution” [11]. In these equations the convolution is defined as

$$P \otimes q = \int_x^1 \frac{dy}{y} P(y) q\left(\frac{x}{y}, \mu^2\right), \tag{9}$$

and the splitting functions are given by

$$\begin{aligned}
\tilde{P}_{qq}(y) &= \frac{P_{qq}(y)}{C_F}; \quad P_{\gamma q}(y) = \frac{P_{gq}(y)}{C_F}; \\
P_{q\gamma}(y) &= \frac{P_{qg}(y)}{T_R}; \quad P_{\gamma\gamma}(y) = \sum_j \frac{-2e_j^2}{3} \delta(1-y) \tag{10}
\end{aligned}$$

We have analogous equations to Eq. (8) for antiquarks. Taking the valence combinations from Eq. (5), we obtain for up and down valence quarks

$$\begin{aligned}
\frac{\partial u^-(x, \mu^2)}{\partial \ln \mu^2} &= \frac{\alpha_s}{2\pi} P_{qq} \otimes u^- + \frac{2\alpha}{9\pi} \tilde{P}_{qq} \otimes u^- ; \\
\frac{\partial d^-(x, \mu^2)}{\partial \ln \mu^2} &= \frac{\alpha_s}{2\pi} P_{qq} \otimes d^- + \frac{\alpha}{18\pi} \tilde{P}_{qq} \otimes d^- \tag{11}
\end{aligned}$$

For the valence CSV parton distributions, since  $\delta u^-(x) = u_p^-(x) - d_n^-(x)$ , from Eq. (11) we obtain the evolution equations for the valence CSV PDFs, to lowest order in  $\alpha_s$  and  $\alpha$ ,

$$\begin{aligned}
\frac{\partial [\delta u^-(x, \mu^2)]}{\partial \ln \mu^2} &\approx \frac{\alpha}{2\pi} (e_u^2 - e_d^2) \tilde{P}_{qq} \otimes u^- ; \\
\frac{\partial [\delta d^-(x, \mu^2)]}{\partial \ln \mu^2} &\approx -\frac{\alpha}{2\pi} (e_u^2 - e_d^2) \tilde{P}_{qq} \otimes d^- . \tag{12}
\end{aligned}$$

Eq. (11) describes how the valence quarks evolve with  $Q^2$  and Eq. (12) shows how the valence CSV

distributions evolve, to lowest order in both  $\alpha_s$  and  $\alpha$ . With increasing  $Q^2$ , partons radiate gluons and photons which carry off momentum. Since the total momentum fraction carried by quarks is given by the second moment of the parton distributions, as  $Q^2$  increases the parton distribution functions will shift towards progressively smaller  $x$  values.

Comparison of Eqs. (11) and (12) shows that the radiation from valence quarks will be greater than that from the valence CSV distributions. This occurs because to lowest order in  $\alpha_s$  and  $\alpha$ , valence quark evolution contains contributions from both gluon and photon radiation, whereas the valence CSV distribution has only a term from photon radiation. This suggests that with increasing  $Q^2$  the valence parton distributions would experience a larger shift to low  $x$  than will the valence CSV distributions. We note that the quantity  $R^-(x)$  defined in Eq. (7) is proportional to the ratio of valence CSV distributions to valence PDFs, at a given  $x$  value. If the CSV valence distributions are becoming larger relative to the valence PDFs at large  $Q^2$ , then we expect the quantity  $R^-(x)$  to grow as  $Q^2$  increases; specifically we would expect the ratio to increase logarithmically with  $Q^2$ .

Eq. (12), the QCD evolution equations for the valence CSV parton distributions, have been solved by Glück *et al.* [12] and also by the MRST group [11]; the two groups made slightly different approximations for the initial conditions. We stress that while the effect of photon radiation is clear, it is far less obvious that the boundary conditions imposed on the calculations are appropriate. That is, we know of no rigorous proof that a low scale, typical of quark models, is the appropriate place to set the effect to zero. In the absence of a compelling theoretical derivation it is extremely helpful to be able to test the idea experimentally.

The MRST group [11] did attempt an experimental test of this method. Including QED radiation in the DGLAP equations introduces a ‘photon parton distribution’  $\gamma(x, Q^2)$ , which appears in Eq. (8). The MRST group attempted to identify this quantity in the process  $ep \rightarrow e\gamma X$  where the final state  $e$  and  $\gamma$  are produced with equal and opposite large transverse momentum. This process has been measured by the ZEUS Collaboration in  $ep$  collisions at  $\sqrt{s} = 300$  and 318 GeV [16]. The observed cross sections were in reasonable agreement with the MRST calculations but disagreed with calculations done using the Monte Carlo simulations PYTHIA [17] and HERWIG

[18]. It would be useful to have other experimental tests of this method for including radiation of photons by partons, and the experiment suggested here could provide additional confirmation of this method.

A second source of valence parton CSV arises naturally from the mass difference between the  $u$  and  $d$  quarks and may be calculated within light cone quark models. In such models the valence quark distribution can be expressed as [19–21]

$$q_v(x, \mu^2) = M \sum_X |\langle X | \frac{1 + \gamma^0 \gamma^3}{2} \psi(0) | N \rangle|^2 \times \delta(M(1-x) - p_X^+) . \quad (13)$$

Eq. (13) denotes the process where a valence quark is removed from a nucleon  $|N\rangle$ , and the result is summed over all final states  $|X\rangle$ . The quantity  $p_X^+$  is the energy of the state following removal of a valence quark with momentum  $k$ . The quantity  $\mu^2$  represents the starting value for the  $Q^2$  evolution of the parton distribution. Eq. (13) is formally exact and provides a natural starting point for calculations which preserve the correct support of the PDFs.

Model quark wavefunctions are found to be nearly invariant under the small mass changes typical of CSV [10], so we concentrate on the breaking of partonic charge symmetry associated with energy shifts resulting from the  $u$  and  $d$  quark mass differences. In particular, we consider the effect of the  $n - p$  mass difference  $\delta M \equiv M_n - M_p = 1.3$  MeV, as well as the difference in diquark masses arising from the current quark mass difference between up and down quarks. We define the quantity

$$\delta \tilde{m} = m_{dd} - m_{uu} , \quad (14)$$

for which we have a robust estimate  $\delta \tilde{m} \sim 4$  MeV [22]. We determine CSV valence PDFs by calculating the variation of quark model parton distributions from Eq. (13) with respect to these quantities, *i.e.*,

$$\delta q_v \approx \frac{\partial q_v}{\partial(\delta \tilde{m})} \delta \tilde{m} + \frac{\partial q_v}{\partial(\delta M)} \delta M . \quad (15)$$

From Eq. (15) the valence charge symmetry violating parton distributions are obtained by taking variations with respect to diquark and nucleon masses on valence parton distributions from quark models. The resulting PDFs account for quark and nucleon mass differences that lead to CSV effects.

Valence CSV parton distributions arising from quark mass difference effects were calculated by Rodionov *et al.* [10]. They used bag model wavefunctions, including the effect of quark mass differences on the quark wave functions as well as on the di-quark and nucleon masses, using Eq. (13). The Rodionov calculation preserved the correct support and included the effect of transverse momentum in the proton. As in any quark model calculation, the resulting leading twist PDFs are appropriate to a relatively low momentum scale (where most of the momentum of the nucleon is carried by valence quarks [21, 23]). In order to compare with experimental data these PDFs are typically evolved up to  $Q^2 = 10$  GeV<sup>2</sup>. We subsequently evolved these parton distributions to the higher  $Q^2$  values appropriate to an electron-ion collider such as the LHeC.

An alternate theoretical approach was due to Sather [9], who investigated the expression for valence parton CSV distributions in a static quark picture. In such models the correct support is no longer guaranteed. In addition, Sather neglected transverse quark momentum. By applying Eq. (15) to Eq. (13) within this approximation scheme, Sather obtained an analytic approximation relating valence quark CSV to derivatives of the valence PDFs. The analytic approximation of Sather is appropriate only at  $Q^2$  values appropriate for quark model calculations, *i.e.*,  $Q^2 \sim 0.25 - 0.5$  GeV<sup>2</sup>.

We used the Sather prescription, differentiating valence parton distribution functions to obtain valence CSV PDFs. For this purpose we used the MRST2001 parton distributions [24] at the starting scale,  $Q_0^2 = 1$  GeV<sup>2</sup>. This is slightly too large a value of  $Q^2$  for the validity of Sather’s analytic approximation, but the resulting errors should be small. We then inserted the resulting CSV PDFs into the DGLAP evolution equations and evolved to the  $Q^2$  appropriate for the electron collider experiments. The results were similar to those obtained using the CSV distributions of Rodionov *et al.*

Since the CSV effects arising from QED splitting effects and from quark mass differences are nearly independent, we have added the two effects to produce a “net” CSV effect.

The quark model estimates of valence parton CSV can be compared with a recent lattice calculation of valence charge symmetry violating parton distributions [25]. The lattice calculation provides

striking confirmation of the quark model results for parton CSV. The lattice calculation was carried out by considering small deviations from the  $SU(3)$  flavor-symmetric point where the strange and light quarks masses are all equal. In that way they could estimate the effects of quark mass differences on parton distributions. The lattice results gave estimates for the second moment of the valence CSV distributions

$$\begin{aligned}\delta U^+ &= \int_0^1 x \delta u^+(x) dx = -0.0023(6) , \\ \delta D^+ &= \int_0^1 x \delta d^+(x) dx = +0.0020(3) .\end{aligned}\quad (16)$$

The lattice results were obtained at a momentum scale  $Q^2 = 4 \text{ GeV}^2$ . Note that the results are appropriate for the  $C$ -even combination of quarks rather than the desired  $C$ -odd combination for valence quarks, because the lattice calculations are sensitive to the  $C$ -even combination. By comparison, the quark model valence quark calculations at a similar scale obtained  $\delta U^- = -0.0014$  and  $\delta D^- = +0.0015$  [10, 26]. Note that the lattice result agrees with the quark model results in both the sign and relative magnitude of the second moment of the valence CSV distributions. The lattice results are 30-50% larger than the quark model values. The differences may result from the inclusion of singlet contributions in the lattice calculations. The lattice results are also in good agreement with the best value obtained for valence quark charge symmetry violation in a phenomenological global fit to high energy data by the MRST group [5]. However, the uncertainties in the lattice calculation are considerably smaller than those from the global fit.

There is one final term that enters into the quantity  $R^-(x)$  of Eq. (7), namely the strange quark momentum asymmetry [27, 28]

$$xs^-(x) \equiv x[s(x) - \bar{s}(x)] . \quad (17)$$

Strange (antistrange) parton distributions can be measured through opposite-sign dimuon production initiated by neutrinos (antineutrinos). A neutrino undergoes a charged-current reaction, producing a  $\mu^-$  and a  $W^+$ , which is absorbed on an  $s$  quark producing a charm quark. The charm quark subsequently undergoes a semileptonic decay producing a  $\mu^+$  and an  $s$  quark. The cross section for this process is proportional to the strange quark distribution. The corresponding reaction initiated by an antineutrino measures the antistrange PDF.

Dimuon cross sections have been measured by the CCFR [29] and NuTeV [30] experiments. From these reactions one can extract the quantity  $xs^-(x)$ . These analyses have been undertaken by five groups: CTEQ [31]; Mason *et al.* [32]; the NNPDF Collaboration [33]; MSTW [34]; and Alekhin, Kulagin and Petti [35]. We used the results of the analysis of Mason *et al.* of the NuTeV neutrino reactions [32]. We made an analytic fit to the best-fit result from Mason *et al.* corresponding to  $Q^2 = 16 \text{ GeV}^2$ . The fit had the form

$$xs^-(x) = Ax^b \exp(-cx)(x - 0.004) . \quad (18)$$

The resulting strange quark asymmetry was inserted into the DGLAP evolution equation and evolved to high  $Q^2$ .

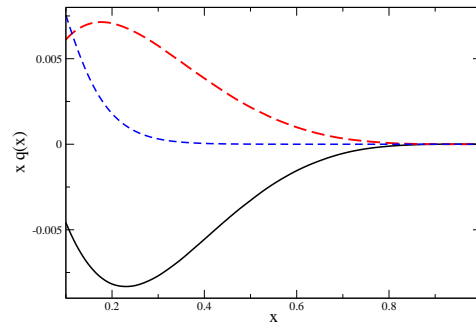


FIG. 3: [color online] Parton distributions that occur in the numerator of Eq. (7). Solid curve:  $x\delta u^-(x)$ ; long-dashed curve:  $x\delta d^-(x)$ ; short-dashed curve:  $xs^-(x)$ . The PDFs have been evolved to  $Q^2 = 10^5 \text{ GeV}^2$ .

The parton distribution functions that occur in the numerator of Eq. (7) are plotted in Fig. 3. The solid curve is  $x\delta u^-(x)$ , the long-dashed curve is  $x\delta d^-(x)$  and the short-dashed curve is  $xs^-(x)$ . As one might expect, the valence CSV distributions peak at a relatively large value  $x \sim 0.2$  while the strange quark asymmetry peaks at an extremely small  $x$  value. Note that due to valence quark normalization, all of these quantities must have zero first moment, *i.e.*,  $\langle q(x) \rangle = 0$ , where  $q = [\delta u^-, \delta d^-, s^-]$ . The strange quark asymmetry has zero first moment because the proton has no net strangeness; the valence CSV distributions must have zero first moment because otherwise this would change the total number of valence

quarks in the neutron. So each of these curves crosses zero at a small value of  $x$  (not shown in Fig. 3).

Another notable point is that the signs of these quantities are such that (for values of  $x$  above the crossover point for all of the parton distributions) all three contributions should add together in the numerator of Eq. (7). Fig. 4 shows the expected value of  $R^-(x)$  vs. Bjorken  $x$ . The solid curve in Fig. 4 includes only the QED splitting contribution to partonic CSV. The long-dashed curve includes both QED splitting and quark mass contributions to valence quark CSV. The short-dashed curve is the result including all three terms in the numerator of Eq. (7), including also the contribution from strange quark asymmetry.

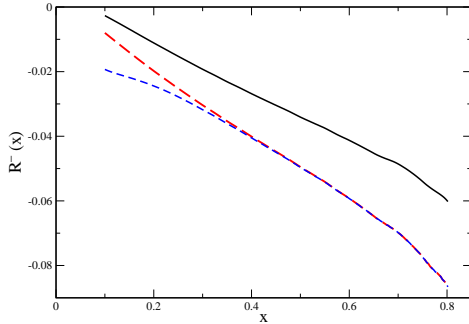


FIG. 4: [color online] Contributions to the quantity  $R^-(x)$  vs.  $x$  from Eq. (7), where the PDFs are evolved to  $Q^2 = 10^5$  GeV<sup>2</sup>. Solid curve: contribution from QED splitting parton CSV term only; long-dashed curve: includes contribution also from quark mass CSV term; short-dashed curve: contribution from all terms including strange quark asymmetry.

We see that for large  $x > 0.2$  the strange quark contribution is essentially negligible. The predicted values of  $R^-(x)$  are large; for  $x = 0.6$  the calculated ratio is greater than 6%. This is quite a sizeable result for partonic CSV terms, which for most observables yield effects at the 1% level or smaller [6]. This confirms our argument that, while both the valence quark and valence CSV distributions shift to lower  $x$  values with increasing  $Q^2$ , the CSV distributions experience a smaller shift (because to lowest order the CSV valence distributions only radiate photons while the valence parton PDFs radiate both gluons and photons), and thus for a given  $x$  the ratio of valence CSV dis-

tributions to valence PDFs should increase slowly with  $Q^2$ . Our best theoretical estimate of the ratio  $R^-(x)$  from Eq. (7) at large  $x$  values is predicted to be rather large, of the order of several percent. For reasonably large values  $x > 0.1$ , the ratio  $R^-(x)$  is composed of relatively equal contributions from valence parton CSV effects arising from quark mass differences and from QED radiation. Thus the quantitative values obtained for the ratio  $R^-(x)$  can provide a further check on the assumptions made in determining charge symmetry violation arising from QED radiation.

In conclusion, a high energy electron/positron collider whose beams interact with deuteron beams from the LHC may produce the most promising observable with which to search for partonic charge symmetry violating effects.

This work was supported in part by the the U.S. National Science Foundation grant NSF PHY-0854805 (JTL) as well as by the Australian Research Council (through an Australian Laureate Fellowship) and the University of Adelaide (AWT).

- 
- [1] E.M. Henley and G.A. Miller, *Mesons in Nuclei*, ed. M. Rho and D.H. Wilkinson, (North-Holland, Amsterdam, 1979), p. 116.
  - [2] G.A. Miller, B.M.K. Nefkens and I. Slaus, Phys. Rept. **194**, 1 (1990).
  - [3] W. Bentz, I. C. Cloet, J. T. Londergan *et al.*, Phys. Lett. **B693**, 462-466 (2010). [arXiv:0908.3198 [nucl-th]].
  - [4] J. T. Londergan, A. W. Thomas, Phys. Rev. **D67**, 111901 (2003). [hep-ph/0303155].
  - [5] A.D. Martin, R.G. Roberts, W.J. Stirling and R.S. Thorne, Eur. Phys. J. **C35**, 325 (2004).
  - [6] J. T. Londergan, J. C. Peng, A. W. Thomas, Rev. Mod. Phys. **82**, 2009-2052 (2010). [arXiv:0907.2352 [hep-ph]].
  - [7] J. T. Londergan and A. W. Thomas, Prog. in Part. Nucl. Phys. **41**, 49 (1998).
  - [8] For details see: <http://www.lhec.org.uk>
  - [9] E. Sather, Phys. Lett. **B274**, 433 (1992).
  - [10] E.N. Rodionov, A.W. Thomas and J.T. Londergan, Mod. Phys. Lett. **A9**, 1799 (1994).
  - [11] A.D. Martin, R.G. Roberts, W.J. Stirling and R.S. Thorne, Eur. Phys. J. **C39**, 155 (2005).
  - [12] M. Glueck, P. Jimenez-Delgado and E. Reya, Phys. Rev. Lett. **95**, 022002 (2005).
  - [13] Y.L. Dokshitzer, Sov. Phys. JETP **46**, 641 (1977).
  - [14] V.N. Gribov and L.N. Lipatov, Sov. J. Nucl. Phys. **15**, 438 (1972).
  - [15] G. Altarelli and G. Parisi, Nucl. Phys. **B146**, 298

- (1977).
- [16] S. Chekanov *et al.* (ZEUS Collaboration), Phys. Lett. B**595**, 86 (2004).
  - [17] T. Sjostrand *et al.*, Comput. Phys. Commun. **135**, 238 (2001).
  - [18] G. Marchesini *et al.*, Comput. Phys. Commun. **67**, 465 (1992).
  - [19] R.L. Jaffe, Nucl. Phys. B**229**, 205 (1983).
  - [20] A.I. Signal and A.W. Thomas, Phys. Rev. D **40**, 2832 (1989).
  - [21] A. W. Schreiber, A. I. Signal, A. W. Thomas, Phys. Rev. D**44**, 2653-2662 (1991).
  - [22] R.P. Bickerstaff and A.W. Thomas, J. Phys. G **15**, 1523 (1989).
  - [23] A. W. Schreiber, A. W. Thomas, J. T. Londergan, Phys. Rev. D**42**, 2226-2236 (1990).
  - [24] A.D. Martin, R.G. Roberts, W.J. Stirling and R.S. Thorne, Eur. Phys. J. C**23**, 73 (2002).
  - [25] R. Horsley, Y. Nakamura, D. Pleiter, P.E.L. Rakow, G. Schierholz, H. Stuben, A.W. Thomas, F. Winter, R.D. Young and J.M. Zanotti, arXiv:1012.0215.
  - [26] J. T. Londergan and A. W. Thomas, Phys. Lett. B**558**, 132 (2003); [hep-ph/0303155].
  - [27] A. I. Signal, A. W. Thomas, Phys. Lett. B**191**, 205 (1987).
  - [28] A. W. Thomas, W. Melnitchouk, F. M. Steffens, Phys. Rev. Lett. **85**, 2892-2894 (2000). [hep-ph/0005043].
  - [29] A.O. Bazarko *et al.* (CCFR Collaboration), Z. Phys. C**65**, 189 (1995).
  - [30] M. Goncharov *et al.* (NuTeV Collaboration), Phys. Rev. D**64**, 112006 (2001).
  - [31] H. L. Lai, P. M. Nadolsky, J. Pumplin, D. Stump, W. K. Tung and C. P. Yuan, JHEP **0704**, 089 (2007).
  - [32] D. Mason *et al.*, Phys. Rev. Lett. **99**, 192001 (2007).
  - [33] R. D. Ball *et al.* [NNPDF Collaboration], Nucl. Phys. B**823**, 195 (2009).
  - [34] A. D. Martin, W. J. Stirling, R. S. Thorne and G. Watt, Eur. Phys. J. C**63**, 189 (2009).
  - [35] S. Alekhin, S. Kulagin and R. Petti, Phys. Lett. B**675**, 433 (2009).